Synthesis and characterization of Ti-27.5Nb alloy made by CLAD® additive manufacturing process for biomedical applications

M. Fischer[1], P. Laheurte[1], P. Acquier[2], D. Joguet[3], L. Peltier[4], T. Petithory[5], K. Anselme[5], P. Mille[6]*

[1] LEM3, Université de Lorraine, Ile du Saulcy, 57045 Metz, France
[2] IREPA Laser, Institut Carnot Mica, Parc d'Innovation, 67400 Illkirch, France
[3] LERMPS, Université de Technologie de Belfort Montbéliard, Sevenans, 90010 Belfort, France
[4] LEM3, Ecole Nationale Supérieure d'Arts et Métiers, 57078 Metz, France
[5] IS2M, CNRS UMR7361, Université de Haute-Alsace, 68057 Mulhouse, France
[6] LGECO Institut National des Sciences Appliquées, 67000 Strasbourg, France

[*] Corresponding author

Abstract

Biocompatible beta-titanium alloys such as Ti-27.5(at.%)Nb are good candidates for implantology and arthroplasty applications as their particular mechanical properties, including low Young's modulus, could significantly reduce the stress-shielding phenomenon usually occurring after surgery. The CLAD® process is a powder blown additive manufacturing process that allows the manufacture of patient specific (i.e. custom) implants. Thus, the use of Ti-27.5(at.%)Nb alloy formed by CLAD® process for biomedical applications as a mean to increase cytocompatibility and mechanical biocompatibility was investigated in this study. The microstructural properties of the CLAD-deposited alloy were studied with optical microscopy and electron back-scattered diffraction (EBSD) analysis. The conservation of the mechanical properties of the Ti-27.5Nb material after the transformation steps (ingot-powder atomisation-CLAD) were verified with tensile tests and appear to remain close to those of reference material. Cytocompatibility of the material and subsequent cell viability tests showed that no cytotoxic elements are released in the medium and that viable cells proliferated well.

Keywords

Beta-titanium, CLAD process, Microstructure, Texture analysis, Mechanical properties, Cytocompatibility, Cell viability

1. Introduction

Elaborated from a combination of non-cytotoxic elements, beta-titanium alloys have been widely studied for applications in biomedical domains [1]. Implantable medical devices should have a

Young's modulus as close as possible to that of the bone (~ 30GPa). Indeed, the durability of a joint replacement or an implant placement depends on the bone remodeling process which is related to the loading conditions of the bone. The stiffness mismatch between implant material and surrounding bone may lead to stress-shielding of the bone as demonstrated by Huiskes et al. [2]. This phenomenon can result in bone resorption and loosening of the implant.

Authors have designed some titanium alloys, for example scanning the proportions of niobium, tantalum, zirconium and molybdenum in Ti-Nb, Ti–Nb–Ta–Zr, Ti–Nb–Ta–Mo and Ti–Nb–Ta–Sn alloys [3]–[6], taking into account the factors of mechanical biocompatibility and non-cytotoxicity. Beta titanium alloys are often studied as an alternative for more « conventional alloys » to improve mechanical biocompatibility [7], [8]. It was shown that beta-titanium alloys such as Ti-27.5(at.%)Nb are excellent candidates for biomedical applications because of their very low elastic modulus (50GPa) close to that of cortical bone (30GPa) and their high strength (600Mpa) [3], [4], [7], [9]–[11]. They could significantly reduce the stress-shielding phenomenon [12]. In addition to the improvement in elastic properties, Ti-Nb alloys are perfectly biocompatible [13] and non-cytotoxic. Their use instead of classical materials such as Ti-6Al-4V or Ti-Ni avoids the release of Al, V and Ni toxic ions in the body [14].

The direct laser deposition process or CLAD® process is a powder blown additive manufacturing process. Its flexibility permits the fabrication of many shapes. It is thus applicable to the production of high added value products such as patient specific implants since it makes the manufacture of shapes close to a patient's morphology possible.

The purpose of this study was to validate the conservation of the particular properties of the Ti-27.5Nb material after the transformation steps as the raw Ti-27.5Nb powder is not available for purchase and has been fully synthesized: pre-alloyed ingot, atomization, laser deposition.

The microstructure of a Ti-27.5Nb wall was analysed by optical microscopy and its phases were identified by X-ray diffraction. Grain growth was studied with EBSD that allowed obtaining a representation of the crystallographic orientations and studying the morphology of the grains. Tensile tests were performed to verify its mechanical properties. Direct and indirect tests were performed to determine cytocompatibility of the material and to evaluate cell viability.

2. Materials and methods

A Ti–27.5(at%)Nb ingot was first melted using the cold crucible levitation melting method using pure metals in weight proportions Ti:Nb=58:42. The ingot obtained was then subjected to a homogenization treatment at 1223 K for 72 ks under high vacuum followed by water quenching. After

that, the material was cold rolled into 2mm x 2mm square section bars. The bars were then hammered into circular section bars before being hot wire drawn. The wire was transformed into powder by the wire-arc atomization method. This method consists in transforming the wire into liquid by plasma generation. Simultaneously, an atomized gas chops the liquid to elaborate particles. The morphology of particles displays a spherical morphology without satellites. Fig 1 and Fig 2 show respectively the powder morphology and size distribution. The average powder size is 66µm and the alloy melting point is close to 2100°C, considerably higher than that of more conventional Ti alloys.

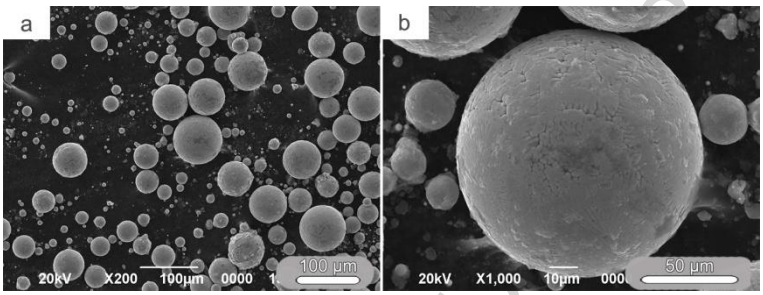

Fig 1: SEM micrograph (at two magnifications) showing the spherical Ti-27.5Nb powder obtained by the wire-arc atomization method

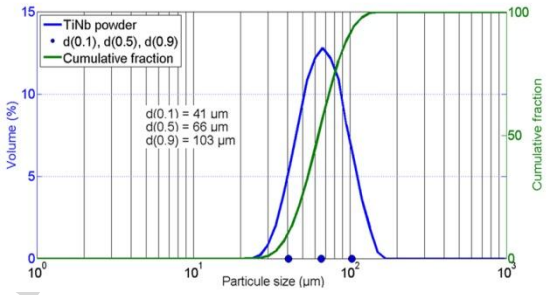

Fig 2: Particle size distribution of particles from wire-arc atomization

The laser deposition tests were carried out on a 5 axis laser metal deposition (LMD) machine designed by IREPA LASER (Fig 3a). The process developed by IREPA LASER is a blown powder additive manufacturing process called CLAD® process, with a laser as the heating source. The metallic powder is injected in a coaxial nozzle, patented by IREPA LASER (US Patent n° 5418350). The powder is carried by argon as transport gas. At the output of the nozzle, the powder jet is shaped by a secondary gas in order to concentrate the powder density (Fig 3b). The powder is then heated and melted by a laser source before being deposited on a substrate. The addition of deposited layers creates the manufactured object.

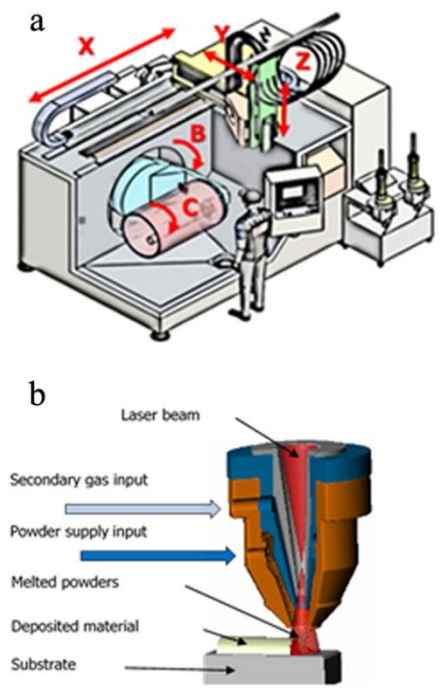

Fig 3: CLAD® machine MAGIC with the 5 axis structure (a) and patented IREPA LASER coaxial deposition nozzle (b)

The machine is equipped with a 500 W fiber laser (optic fiber Ø200 µm, λ = 1070 nm). This machine called MAGIC has a continuous 5 axis configuration and a working envelope of X1500 × Y800 × Z800 mm for the linear axis, and a swiveling (B) and rotating (C) movement for the part. The nozzle is fitted on the linear axis and works always vertically because the gravity affects the powder jet stream. Two nozzles (US Patent n° 5418350) are integrated into this machine and work alternatively for the manufacturing of the parts. The first nozzle (called macroCLAD 10Vx) makes deposition tracks with a width in the range of 1-1.2 mm, and the second nozzle (called macroCLAD 24Vx), equipped with a different optical system, makes tracks width in the range of 2-2.4 mm. At last the machine is equipped with a gas enclosure with a volume of 12 m^3, specially adapted for the manufacturing of Ti alloys parts, and able to work with O_2 level lower than 40ppm, and H_2O level lower than 50ppm. Indeed, after first argon filling, the machine works with a closed-circuit of argon continuously purified allowing very low oxygen partial pressure. Processing parameters are summarized in Table 1.

Table 1: LMD processing parameters

Laser power	500W
Spot diameter	700µm
Deposition speed	1000mm/min
Powder flow	4g/min

The powder obtained from wire-arc atomization was used in the CLAD® process with the macroCLAD 10Vx nozzle to manufacture Ti-27.5Nb walls with dimensions height x width x thickness 100 mm x 70 mm x 2 mm. They were produced by depositing two adjacent tracks per layer.

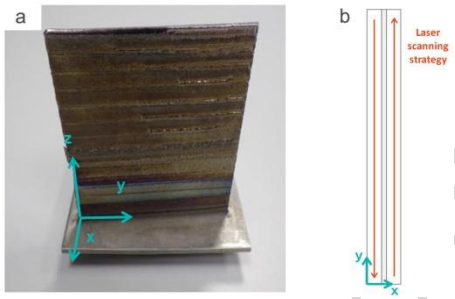

Fig. 4: (a.) manufactured wall and (b.) its fabrication scanning strategy

The chemical composition of Ti-27.5Nb wire drawn material as well as Ti-27.5Nb powder and Ti-27.5Nb CLAD® wall is presented in Table 2. The titanium and niobium contents were measured by inductively coupled plasma atomic emission spectroscopy. The carbon and the oxygen were analyzed by fusion method and infrared detection, and the nitrogen and the hydrogen by fusion and conduction. Most of the oxygen present in the final part is due to the atomization process inducing high levels of oxygen in the powder. There is a partial desorption of this oxygen during the fusion of the powder in the LMD process. As comparison with a more common material, oxygen levels allowed in Ti6Al4V ELI are 1300ppm (ASTM F136 and ASTM F3001-14) and in Ti-6Al-4V are 2000ppm (ASTM F2924-14).

Table 2: Chemical composition (wt. %) of the powder mix

Element	**Ti**	**Nb**	**C**	**H**	**N**	**O**
Incertitude (wt. %)	(±1)	(±1)	(±0.003)	(±0.0012)	(±0.0020)	(±0.020)
Wire (wt. %)	58	42	0.014	0.0053	0.0160	0.147
Powder (wt. %)	58	42	0.020	0.0160	0.0630	0.789
Wall (wt. %)	57	43	0.022	0.0138	0.0375	0.323

The microstructure of the Ti-27.5Nb walls was analysed by optical microscopy after grinding and etching with Kroll's reagent and phases were identified by X-ray diffraction using a Cu Kα source (λ=0.1540 nm). Grain growth was studied with EBSD analyses showing a representation of the crystallographic orientations and the morphology of the grains.

Tensile tests were performed to verify the mechanical properties of the deposited alloy. Six tensile specimens were machined from a wall in the longitudinal direction. Half the specimens were tested as-build (AB) and the others were solution treated at 1173 K for 3.6 ks followed by water quenching ($ST_{CLAD®}$). Wire drawn material (from ingot) was tested as well for reference: three wire specimens with diameter 2 mm were sampled after the hot wire drawing process. Specimens were subsequently solution treated (ST_{ref}) at 1173 K for 3.6 ks under Ar atmosphere and water quenched. Tensile tests were performed at 20°C, with 20mm in gauge length at a constant strain rate of $0.05min^{-1}$.

Cytocompatibility tests were performed in order to verify the safety of the Ti-27.5Nb alloy before and after CLAD® process. Indirect and direct tests were performed following the ISO10993-5 standard [15]. First, extraction media were produced for indirect tests by immersion of raw powder, wire or bars of Ti-27.5Nb in Dulbecco's modified Eagle cell culture medium without fetal bovine serum (FBS) addition. A deep cleaning was needed before immersion of materials in order to remove any pollution from the post-processing protocols. Samples were immersed in successive 10 minutes baths in ultrasounds of chloroform, acetone, ethanol and distilled water. After cleaning, samples were sterilized at 180°C in air during 2 hours and immersed in culture medium during 1, 3 or 5 days at 37°C in a 5% CO_2 atmosphere in a cell culture incubator. Afterwards, immersion media were harvested and kept at -20°C. Immediately before use, they were thawed, completed with 10% FBS and deposited for 24 hours on human mesenchymal stromal cells (STRO-$1A^+$ cells) [16] cultured at confluence in 96-well plates. After this time, viability of cells was quantified in each well using a MTT test.

Secondly, STRO-$1A^+$ cells were directly inoculated on samples prepared from walls manufactured by CLAD® from Ti-27.5Nb powder. Walls were cut in $1cm^2$ pieces and mirror-polished. Viability and proliferation of cells after 4 hours, 24 hours, 3 days and 6 days were quantified by the PrestoBlue® cell viability reagent (ThermoFisher Scientific, France) and compared on unpolished and mirror-polished samples. Cells were inoculated at 2.10^4 cells / sample. After 1 and 3 days of culture, samples were prepared for cell morphology examination by confocal microscopy. They were fixed with paraformaldehyde 2% and stained with Hoechst 33342 (Sigma Aldrich) for revealing cell nucleus and Alexa555-phalloidin (Thermofisher Scientific, France) for staining actin cytoskeleton. The examination was performed thanks to a Zeiss LSM700 upright confocal microscope.

Standard statistical analyses (Student t-test) were performed to compare the number of viable cells adhering on the different samples at the various culture times.

3. Results and discussion

It was essential to analyze the properties of the transformed material in order to determine whether the properties of the bulk (ST_{ref}) material were retained.

3.1. Microstructure and phase analysis

On the micrograph Fig. 5, the superposition of the deposited layers is visible and the two adjacent tracks are discernible. The width and height of each track is estimated to be respectively 1.2mm and 0.3mm. Nonetheless, the two scanning tracks seem asymmetrical. This is due to the fact that in order to obtain a compact deposit, an overlapping of 30% is required between two successive tracks.

At higher magnification, the dendritic solidification structure can be observed.

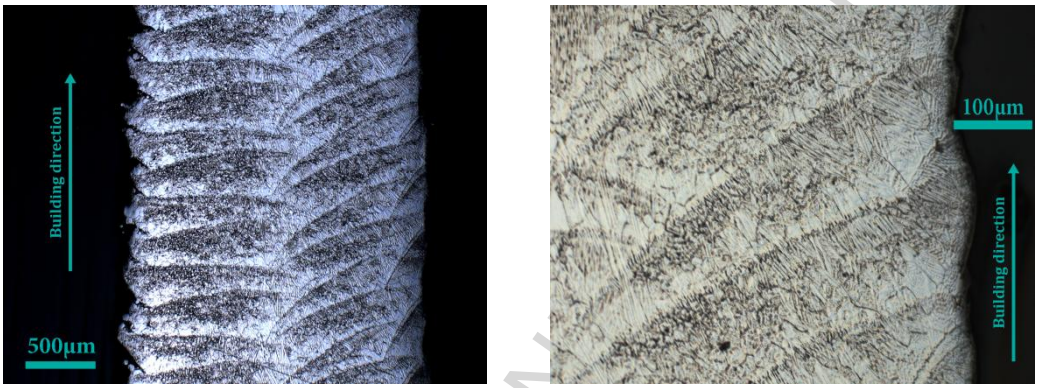

Fig. 5: Optical micrograph showing the solidification structure of the Ti-27.5Nb alloy after CLAD® in the plane (xz)

Ti–27.5Nb gas atomized powder and Ti-27.5Nb CLAD® AB processed sample exhibit only ß-phase peaks in XRD (Fig. 6) (Cu Kα irradiation) in agreement with the high cooling rates occurring during the process. The intensity of the peaks of the powder diffractogram and that of the CLAD® sample are identical. This shows the absence of texture in the processed material.

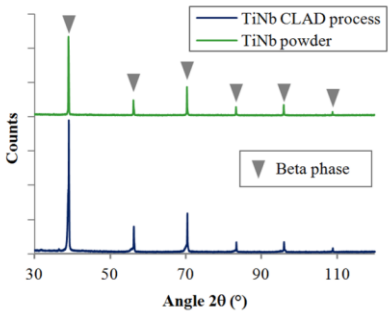

Fig. 6: X-ray diffraction profiles of Ti-27.5Nb powder and Ti27.5Nb after CLAD® process

EBSD analyses were conducted in order to further highlight the grain morphology. The growth rate, temperature gradient, melt pool shape, travel speed and alloy constitution will all control the final microstructure of a solidifying melt pool. As can be seen in Fig. 7, representing the IPFZ (inverse pole

figure) EBSD map of the complete thickness of the wall, the deposited alloy is entirely composed of large beta grains. Contrary to what can be observed for some other laser deposited titanium alloys, the beta structure is not columnar. Indeed, laser deposited Ti-6Al-4V for example, usually presents a full α' phase with vertical prior columnar beta grains [17], [18]. Here, the beta grains present different morphologies depending on their location. Indeed, on the sides (near the faces of the wall), large elongated beta grains can mainly be found whereas in the core of the wall, there are mainly smaller equiaxed beta grains. Moreover, there is a difference between the two sides of the map. Indeed, on the right, the grains are elongated and have an inclination of approximately 45° with respect to the face of the wall. On the left, the grains are also elongated but are perpendicular to the face of the wall.

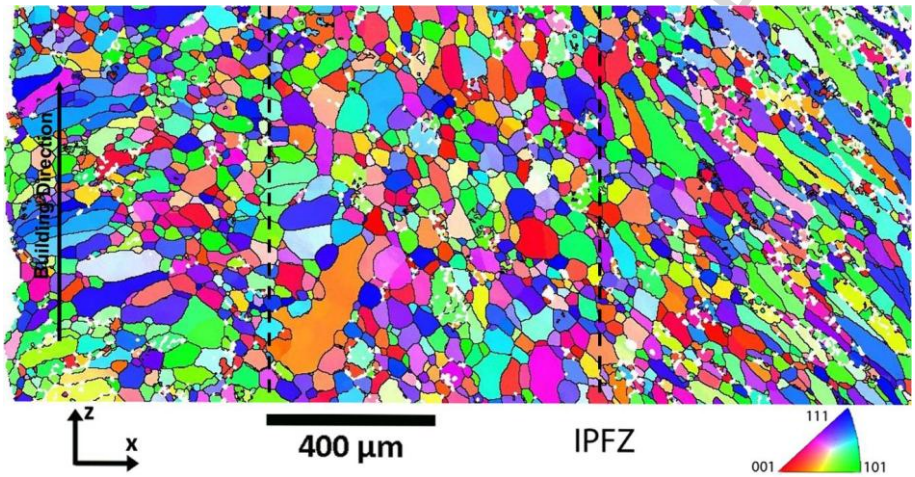

Fig. 7: EBSD analysis on the width of the wall

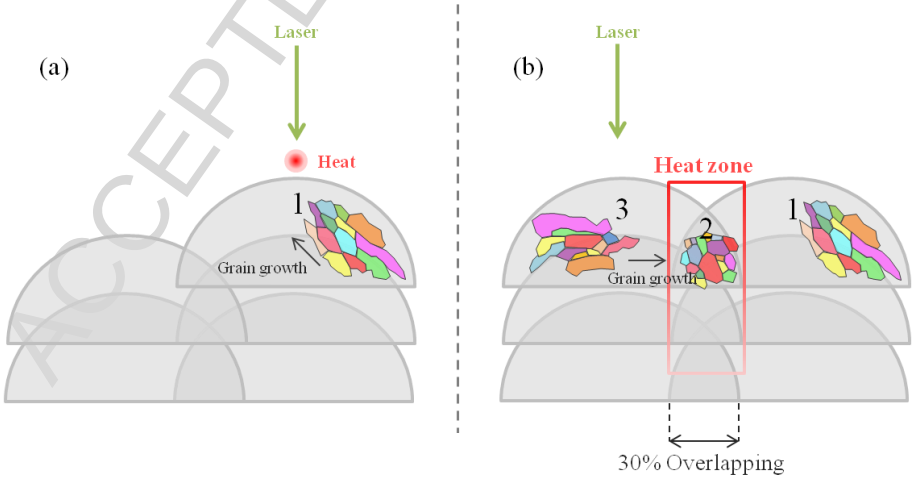

Fig. 8: Grain growth during the melting-remelting-solidification process occurring during the first (a) and second (b) deposition tracks in CLAD®

The different grain morphologies are due to varying cooling speeds and thermal phenomenon related to the fabrication strategy. Because the deposit was made for the first track scanning from the front to

the back and the other way around for the second (from the back to the front), the thermal phenomenon happening is different from one side to the other. When the first track is deposited, there is a directional solidification of the grains towards the direction of the heat i.e. the direction of the moving laser (Fig. 8(a) index 1). When the second track is deposited, two areas are to be distinguished (2 and 3 on Fig. 8(b)). The area indexed 2 corresponds to the overlapping of the tracks, thus a mix between remelted metal from the first track and freshly deposited metal from the second track. In this zone, there is no directional solidification because temperature is homogeneous in the core of the wall. It forms a heat zone where the grains grow in an equiaxial shape, analogous to the center of a cooling ingot [19], [20]. The area indexed 3 consists of the main part of the second track. Here, there is a directional solidification perpendicular to the edge, in the direction of the heat zone in the core of the wall (2 in Fig. 8(b)).

The final microstructure of a Ti-27.5Nb CLAD® part will depend on its geometry. It is highly probable that a larger part, built from many adjacent tracks and thus more similar to the center of the wall will mostly contain equiaxed beta grains.

The EBSD analyses were performed in a significantly large portion of the CLAD® Ti-27.5Nb wall and highlight the absence of preferential crystallographic orientation of the grains.

3.2. Mechanical characterization

One of the main advantages regarding the use of a Ti-27.5Nb alloy for biomedical applications is its low elastic modulus [21], [22]. The properties of the wall built by CLAD® process were tested by loading-unloading tensile tests with imposed strain increasing by 1% for as-built samples (AB) and for solution treated samples ($ST_{CLAD®}$) and compared to the reference (ST_{ref}) (Fig. 9).

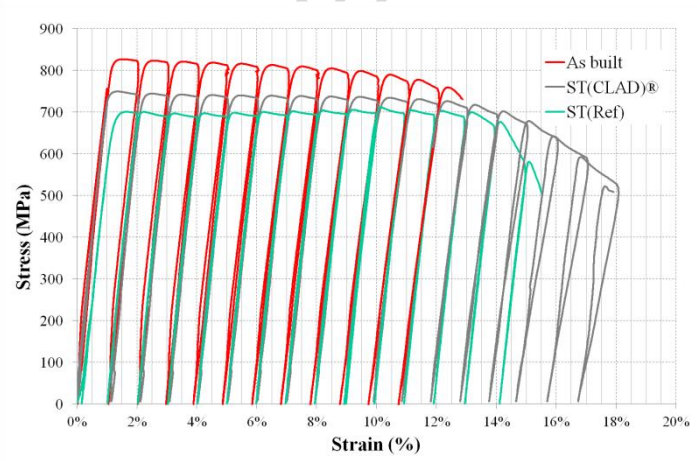

	$\sigma_{0.2}$ (Mpa)	σ_{max} (Mpa)	E (Gpa)	$\frac{\sigma_{0.2}}{E}$
ST_{Ref}	650±4	700±4	65±4	10
As built	800±5	820±5	70±3	11.4
$ST_{CLAD®}$	750±4	750±4	70±4	10.7

Fig. 9: Stress-strain curves for Ti-27.5Nb CLAD® samples AB, $ST_{CLAD®}$ and for reference sample ST_{ref}

For the three metallurgical states, similar mechanical behavior is observed with no superelasticity, similarly to that observed by Kim et al. [5] in Ti-*x*Nb alloys with *x* superior to 27%.

The elastic moduli and ultimate tensile strengths obtained from the stress-strain curves are respectively 70GPa±3GPa and 820MPa±5MPa for the AB sample and 70GPa±4GPa and 750MPa±4MPa for the $ST_{CLAD®}$ sample. There is very little difference between the two states which confirms the high cooling rates in CLAD® PROCESS.

However, the moduli and ultimate tensile strengths of these LMD samples are higher than that of the ST_{ref} that has a modulus of 65GPa±4GPa and ultimate tensile strength of 700MPa±5MPa. This gap can be explained by a presence of oxygen in the CLAD® samples: 3500ppm i.e. 1.3at.%O (Table 2). Indeed, many studies have compared Ti-Nb-O alloys with addition of 0.5% to 2% oxygen to Ti-Nb alloys.

Wei et al [23] investigated the influence of oxygen content in beta-titanium alloys and in particular in Ti-Nb-Zr-Ta-(0-2at.%)O. The experimental results highlighted an apparent change in stress-strain behaviors with increasing oxygen. Ultimate tensile strength was increased by 30% to 60% of its original value; Young's modulus increased gradually from 56GPa (0%O) to 90GPa (2%O) but remaining around 60GPa between 0.5%O and 1.5%O; elongation remained high until addition of 1%O; superelastic behavior was suppressed with any addition of oxygen. They concluded that the best behavior for biomedical applications was obtained with Ti-22.5Nb-0.7Zr-2Ta-1O.

Nii at al. and Tahara et al [24], [25] worked on oxygen addition in Ti-26Nb alloy. Both demonstrated a change of the stress-strain curves by the addition of 1%at.%O to the Ti-26Nb alloy : ultimate tensile strength (UTS) increased from around 300MPa to 700MPa and no martensitic transformation was observed. In fact, the martensitic start transformation (Ms) was proven to decrease by 160K with 1at.% increase of oxygen content [26], [27] thus preventing the transformation at ambient temperature and stabilizing the beta phase in beta-titanium alloys.

Hence, both yield strength and ultimate tensile strength increase with the addition of O. Oxygen strengthens the material and decreases its superelastic properties. Moreover, the amount of oxygen can be critical for martensitic phase transformations in Ti alloys because Ms temperature decreases with increasing oxygen content. From these points of view it is important to keep the oxygen content as low as possible. In our case, there was a significant presence of oxygen after the atomization process that can be explained by the small size and the high reactivity of the powder particles. There is around 3500ppm oxygen in the deposited alloy which corresponds to approximately 1.3at.%O. This explains the difference with the reference ST Ti-27.5Nb alloy. Nonetheless, the oxygen amount in the deposited material is lower than that contained in the powder. During fusion, desorption of oxygen occurs.

3.3. *Cytocompatibility analysis*

The indirect cytotoxicity tests confirmed that neither powders, wires nor bars released any cytotoxic elements after 1, 3 or 5 days of immersion in extraction medium (data not shown).

When the cells were directly cultured on unpolished or polished CLAD® Ti-27.5Nb samples, adhesion and proliferation of cells were maintained and even improved after 3 days on polished samples compared to control (polystyrene cell culture dishes). Proliferation was significantly higher on polished samples compared to unpolished CLAD® ones from 24h to 6 days (Fig. 10). That confirms previous works that demonstrated the cytocompatibility of pure niobium and Ti-Nb alloys [13], [28]–[30]. The morphology of cells after 24 hours confirmed the good adhesion of cells on both Ti-27.5Nb surfaces. On unpolished samples, cells logically aligned following surface texture due to CLAD® process as previously observed in a lot of published studies reviewed by Anselme and Bigerelle [6] (Fig. 11).

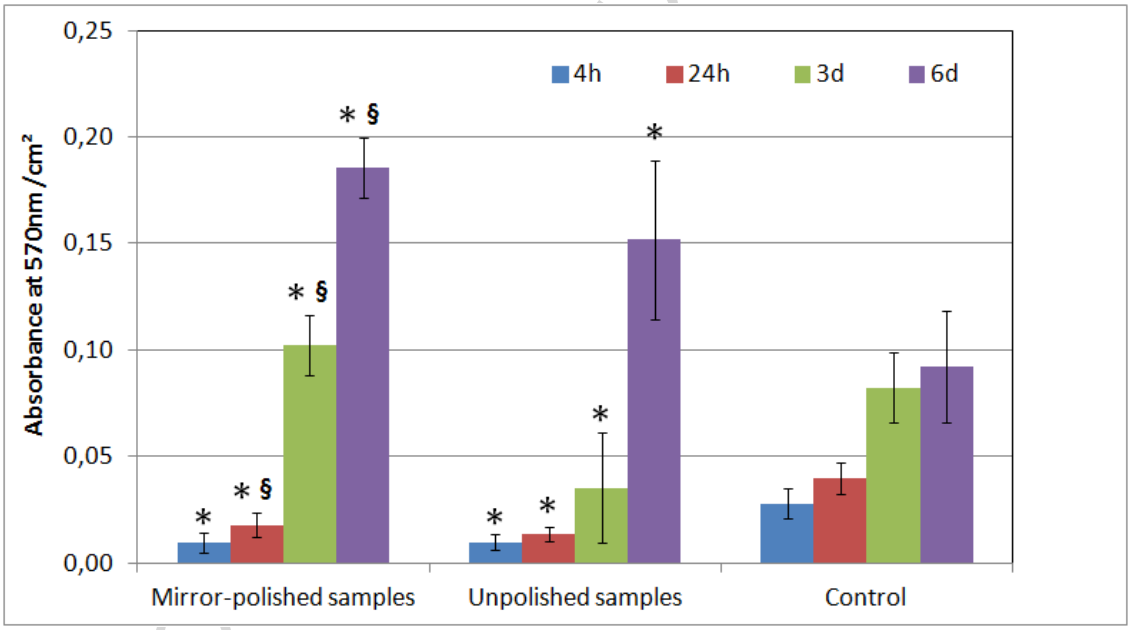

*Fig. 10: Viability of cells cultured on mirror-polished and unpolished CLAD®-treated Ti-27.5Nb samples is quantified over 6 days thanks to PrestoBlue® cell viability reagent. Absorbance was measured at 570 nm and normalized to sample surface. Control is polystyrene of cell culture dishes. * Statistically different from control, $p<0.05$. § Statistically different from unpolished CLAD®-treated Ti-27.5Nb samples, $p<0.05$*

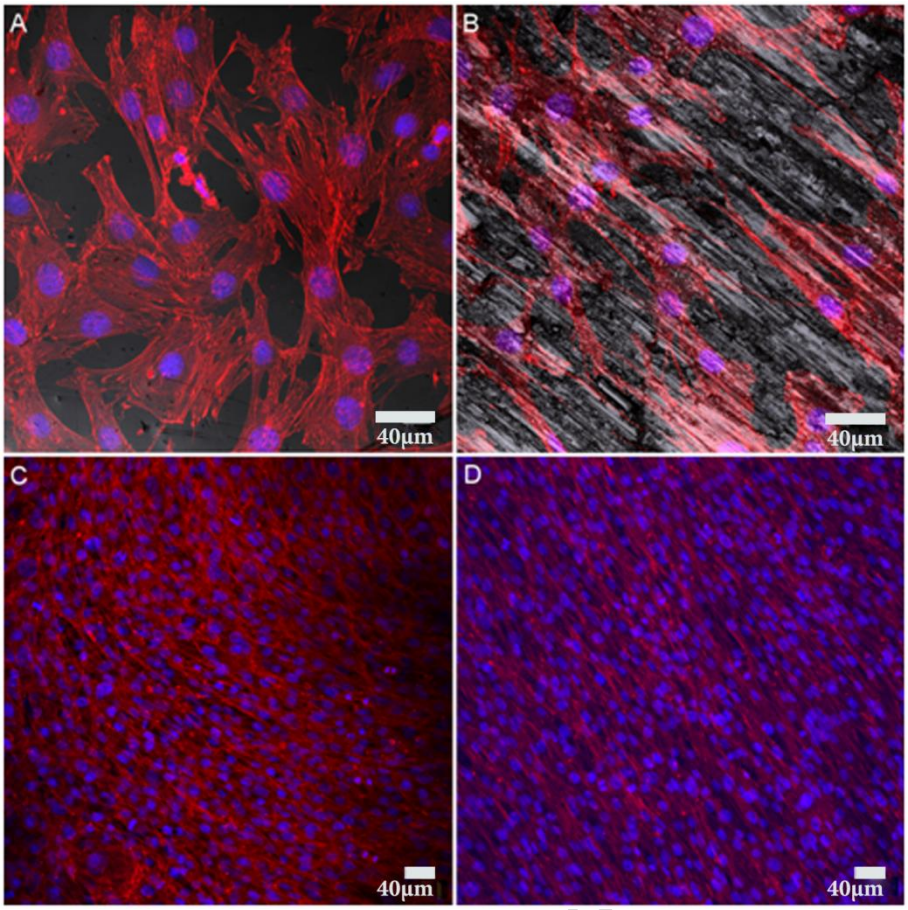

Fig. 11: Morphology of cells cultured 24 hours (A,B) and 3 days (C,D) on mirror-polished (A,C) and unpolished (B,D) CLAD®-treated Ti-27.5Nb samples.

Conclusion

The goal of this study was to synthesize and characterize a CLAD-deposited Ti-27.5Nb alloy. From Ti-27.5Nb ingots, wire was obtained and transformed into spherical powder by wire-arc atomization method. Samples were manufactured by CLAD deposition. We demonstrated that:

- Wall contains more oxygen than ingot but less than powder.
- The produced sample is fully beta with no crystallographic texture.
- Grain morphology highly depends on thermal history and hence on part geometry.
- Young's modulus and ultimate tensile strength is higher for as-built CLAD samples than for ST_{Ref} samples. The ratio $\frac{\sigma_{0.2}}{E}$,i.e. the elastic strain is more advantageous for the deposited material.
- Material did not hinder cell growth and viability of cells. Results were even better with polished samples.

Most of the initial properties of this alloy are preserved or even enhanced after the deposition process.

Acknowledgements

The authors gratefully acknowledge the financial support of The French National Research Agency, project ID ANR-12-EMMA-0003.

Bibliography

[1] M. Niinomi, "Mechanical biocompatibilities of titanium alloys for biomedical applications.," *J. Mech. Behav. Biomed. Mater.*, vol. 1, no. 1, pp. 30–42, Jan. 2008.

[2] R. Huiskes, H. Weinans, and B. Van Rietbergen, "The Relationship Between Stress Shielding and Bone Resorption Around Total Hip Stems and the Effects of Flexible Materials," *Clin. Orthop. Relat. Res.*, vol. NA;, no. 274, pp. 124–134, 1992.

[3] D. Kuroda, M. Niinomi, M. Morinaga, Y. Kato, and T. Yashiro, "Design and mechanical properties of new β type titanium alloys for implant materials," *Mater. Sci. Eng. A*, vol. 243, no. 1–2, pp. 244–249, Mar. 1998.

[4] W. Elmay, P. Laheurte, A. Eberhardt, B. Bolle, T. Gloriant, E. Patoor, F. Prima, D. Laille, P. Castany, and M. Wary, "Stability and elastic properties of Ti-alloys for biomedical application designed with electronic parameters," *EPJ Web of Conference*, 2010. .

[5] H. Y. Kim, Y. Ikehara, J. I. Kim, H. Hosoda, and S. Miyazaki, "Martensitic transformation, shape memory effect and superelasticity of Ti–Nb binary alloys," *Acta Mater.*, vol. 54, no. 9, pp. 2419–2429, May 2006.

[6] H. Y. Kim, S. Hashimoto, J. Il Kim, H. Hosoda, and S. Miyazaki, "Mechanical Properties and Shape Memory Behavior of Ti-Nb Alloys," *Mater. Trans.*, vol. 45, no. 7, pp. 2443–2448, 2004.

[7] M. Niinomi, M. Nakai, and J. Hieda, "Development of new metallic alloys for biomedical applications.," *Acta Biomater.*, vol. 8, no. 11, pp. 3888–903, Nov. 2012.

[8] M. Fischer, D. Joguet, G. Robin, L. Peltier, and P. Laheurte, "In situ elaboration of a binary Ti–26Nb alloy by selective laser melting of elemental titanium and niobium mixed powders," *Mater. Sci. Eng. C*, Feb. 2016.

[9] F. Sun, S. Nowak, T. Gloriant, P. Laheurte, A. Eberhardt, and F. Prima, "Influence of a short thermal treatment on the superelastic properties of a titanium-based alloy," *Scr. Mater.*, vol. 63, no. 11, pp. 1053–1056, Nov. 2010.

[10] W. Elmay, F. Prima, T. Gloriant, B. Bolle, Y. Zhong, E. Patoor, and P. Laheurte, "Effects of thermomechanical process on the microstructure and mechanical properties of a fully martensitic titanium-based biomedical alloy.," *J. Mech. Behav. Biomed. Mater.*, vol. 18, pp. 47–56, Feb. 2013.

[11] Y. L. Hao, S. J. Li, S. Y. Sun, and R. Yang, "Effect of Zr and Sn on Young's modulus and superelasticity of Ti–Nb-based alloys," *Mater. Sci. Eng. A*, vol. 441, no. 1–2, pp. 112–118, Dec. 2006.

[12] B. Piotrowski, A. A. Baptista, E. Patoor, P. Bravetti, A. Eberhardt, and P. Laheurte, "Interaction of bone-dental implant with new ultra low modulus alloy using a numerical approach.," *Mater. Sci. Eng. C. Mater. Biol. Appl.*, vol. 38, pp. 151–60, May 2014.

[13] R. E. McMahon, J. Ma, S. V Verkhoturov, D. Munoz-Pinto, I. Karaman, F. Rubitschek, H. J. Maier, and M. S. Hahn, "A comparative study of the cytotoxicity and corrosion resistance of nickel-titanium and titanium-niobium shape memory alloys.," *Acta Biomater.*, vol. 8, no. 7, pp. 2863–70, Jul. 2012.

[14] S. G. Steinemann, "Metal implants and surface reactions," *Injury*, vol. 27, p. S/C16-S/C22, Jan. 1996.

[15] "ISO 10993-5:2009 - Biological evaluation of medical devices -- Part 5: Tests for in vitro cytotoxicity." .

[16] B. O. Oyajobi, A. Lomri, M. Hott, and P. J. Marie, "Isolation and characterization of human clonogenic osteoblast progenitors immunoselected from fetal bone marrow stroma using STRO-1 monoclonal antibody.," *J. Bone Miner. Res.*, vol. 14, no. 3, pp. 351–61, Mar. 1999.

[17] T. Wang, Y. Y. Zhu, S. Q. Zhang, H. B. Tang, and H. M. Wang, "Grain Morphology Evolution Behaviors of Titanium Alloy Components by Laser Melting Deposition Additive Manufacturing," *J. Alloys Compd.*, vol. 632, pp. 505–513, Feb. 2015.

[18] B. E. Carroll, T. A. Palmer, and A. M. Beese, "Anisotropic tensile behavior of Ti–6Al–4V components fabricated with directed energy deposition additive manufacturing," *Acta Mater.*, vol. 87, pp. 309–320, Apr. 2015.

[19] M. G. Glavicic, P. A. Kobryn, F. Spadafora, and S. L. Semiatin, "Texture evolution in vacuum arc remelted ingots of Ti-6Al-4V," *Mater. Sci. Eng. A*, vol. 346, no. 1–2, pp. 8–18, Apr. 2003.

[20] G. L. Chen, X. J. Xu, Z. K. Teng, Y. L. Wang, and J. P. Lin, "Microsegregation in high Nb containing TiAl alloy ingots beyond laboratory scale," *Intermetallics*, vol. 15, no. 5–6, pp. 625–631, May 2007.

[21] W. Elmay, E. Patoor, B. Bolle, T. Gloriant, F. Prima, A. Eberhardt, and P. Laheurte,

"Modification par traitements thermo-mécaniques des propriétés élastiques d ' alliages binaires Ti-Nb pour les applications biomédicales," in *Congrès français de mécanique*, 2011, pp. 1–6.

[22] W. Elmay, E. Patoor, T. Gloriant, F. Prima, and P. Laheurte, "Improvement of Superelastic Performance of Ti-Nb Binary Alloys for Biomedical Applications," *J. Mater. Eng. Perform.*, vol. 23, no. 7, pp. 2471–2476, 2014.

[23] Q. Wei, L. Wang, Y. Fu, J. Qin, W. Lu, and D. Zhang, "Influence of oxygen content on microstructure and mechanical properties of Ti–Nb–Ta–Zr alloy," *Mater. Des.*, vol. 32, no. 5, pp. 2934–2939, May 2011.

[24] Y. Nii, T.-H. Arima, H. Y. Kim, and S. Miyazaki, "Effect of randomness on ferroelastic transitions: Disorder induced hysteresis loop rounding in Ti-Nb-O martensitic alloy.pdf," *Physical Review B*, 2010. .

[25] M. Tahara, Y. K. Kim, T. Inamura, H. Hosoda, and S. Miyazaki, "Role of interstitial atoms in the microstructure and non-linear elastic deformation behavior of Ti-Nb alloy," *Journal of Alloys and Compounds*, 2013. .

[26] J. Il Kim, H. Y. Kim, H. Hosoda, and S. Miyazaki, "Shape Memory Behavior of Ti–22Nb–(0.5–2.0)O(at%) Biomedical Alloys," *Mater. Trans.*, vol. 46, no. 4, pp. 852–857, 2005.

[27] S. Miyazaki, H. Y. Kim, and H. Hosoda, "Development and characterization of Ni-free Ti-base shape memory and superelastic alloys," *Mater. Sci. Eng. A*, vol. 438–440, pp. 18–24, Nov. 2006.

[28] E. Eisenbarth, D. Velten, M. Müller, R. Thull, and J. Breme, "Biocompatibility of beta-stabilizing elements of titanium alloys," *Biomaterials*, vol. 25, no. 26, pp. 5705–13, Nov. 2004.

[29] Y.-J. Park, Y.-H. Song, J.-H. An, H.-J. Song, and K. J. Anusavice, "Cytocompatibility of pure metals and experimental binary titanium alloys for implant materials," *J. Dent.*, vol. 41, no. 12, pp. 1251–8, Dec. 2013.

[30] K. Anselme and M. Bigerelle, "Role of materials surface topography on mammalian cell response," *Int. Mater. Rev.*, vol. 56, no. 4, pp. 243–266, Jul. 2011.

Highlights

Biomimetic implants can be provided from additive manufacturing with beta-titanium alloys

We studied the properties of a Ti-Nb alloy elaborated with a laser deposition process

TiNb alloy processed by LMD consists of only beta phase due to rapid cooling

No preferential crystallographic texture is observed with EBSD analyses

TiNb samples showed a combination of high strength and low Young's modulus